Chemistry of Heterocyclic Compounds **2020**, *56*(6), 747–755

Synthesis and biological evaluation of novel dispiro compounds based on 5-arylidenehydantoins and isatins as inhibitors of p53–MDM2 protein–protein interaction

Anastasia Beloglazkina[1], Alexander Barashkin[1], Vladislav Polyakov[1], German Kotovsky[1], Nikita Karpov[1], Sofia Mefedova[1], Bogdan Zagribelny[1,2], Yan Ivanenkov[2], Marina Kalinina[3], Dmitry Skvortsov[1,4], Victor Tafeenko[1], Nikolay Zyk[1], Alexander Majouga[1,5,6], Elena Beloglazkina[1]*

[1] *Lomonosov Moscow State University, 1 Build. 3 Leninskie Gory, Moscow 119991, Russia; e-mail: bel@org.chem.msu.ru*

[2] *Moscow Institute of Physics and Technology (State University), 9 Institutskiy Pereulok, Dolgoprudny 141700, Moscow Region, Russia*

[3] *Skolkovo Institute of Science and Technology, 4 Alfred Nobel St., Skolkovo 143025, Russia*

[4] *Faculty of Biology and Biotechnologies, Higher School of Economics, 7 Vavilova St., Moscow 117312, Russia*

[5] *National University of Science and Technology MISiS, 9 Leninsky Ave., Moscow 119049, Russia*

[6] *D. Mendeleev University of Chemical Technology of Russia, 9 Miusskaya Sq., Moscow 125047, Russia*

Published in Khimiya Geterotsiklicheskikh Soedinenii, 2020, *56*(6), 747–755

Submitted February 17, 2020
Accepted March 2, 2020

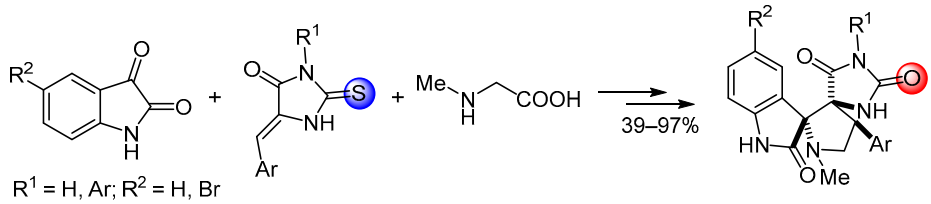

R^1 = H, Ar; R^2 = H, Br

A series of novel hydantoin-based dispiroindolinones as potential small-molecule inhibitors of p53–MDM2 protein–protein interaction were synthesized by two methods, using 2-arylidenehydantoins as starting materials. Some compounds demonstrate moderate cytotoxicity against cancer cell lines with IC_{50} in micromolar concentration range, which is comparable to nutlin-3. Two of the synthesized dispiroindolinones show p53-related activity in p53 reporter activation test.

Keywords: hydantoins, spirooxindole, anticancer drugs, 1,3-dipolar cycloaddition, p53–MDM2 inhibitors.

During the past few years, an increasing interest for nonpeptide small-molecule compounds inhibiting the p53–MDM2 protein–protein interaction of cell proteins has been observed.[1] The p53 protein is a tumor suppressor which plays a key role in cell life cycle and apoptosis, and MDM2 protein is its endogenous inhibitor.[2,3] If this protein–protein interaction is blocked, the released p53 can activate the process of tumor destruction, which may be used in the anticancer therapy. In many types of human cancer cell lines, p53 is mutated and inactivated, which implies the importance of disabling p53 function.[4] Some strategies have been used for the correction of p53-related regulatory pathway dysfunction, for example, small-molecule inhibitors of p53–MDM2 interaction, p53 gene therapies, and drugs targeting chaperones, which bind to mutant p53 and restore its functions.[5]

It is known that MDM2 protein has two binding sites (so-called site 1 and site 2)[5] and both sites are equally probable targets for small-molecule inhibitors. The structural basis of p53–MDM2 protein–protein interaction, which was established by X-ray crystallography,[6] is primarily related with three hydrophobic residues Phe19, Trp23, and Leu26 from the R-helix in p53 and a small, but deep pocket in MDM2. To inhibit their interaction, it is necessary to design a rigid core structure of small-molecule inhibitor, which can build-in to the hydrophobic region of MDM2.

0009-3122/20/56(6)-0747©2020 Springer Science+Business Media, LLC

The anticancer compound nutlin-3,[7] which currently undegoes clinical trials, is one of the most known inhibitors of the p53–MDM2 protein–protein interaction; this compound is able to bind to the p53–MDM2 pocket and inhibit this protein interaction in nanomolar concentrations.[7] Treatment of cancer cells expressing wild-type p53 with nutlin-3a induced nongenotoxic stabilization of p53 protein and subsequent activation of a p53 pathway, which was translated *in vivo* to a reduction in xenograft mice tumor.[8] The molecule of nutlin-3a, which definitely binds to the site 1 of MDM2 protein, may be a template for the design of new p53–MDM2 inhibitor molecules.[9]

Since the indole ring of Trp23 residue of p53 is located deep inside a hydrophobic pocket of MDM2 and its NH group forms a hydrogen bond with the backbone carbonyl in MDM2, Trp23 appears to be most crucial for binding of p53 to MDM2. Previously,[5,10] Wang's group searched for chemical moieties that can mimic the Trp23 interaction with MDM2. In addition to the indole ring itself, they have found that oxindole can perfectly mimic the side chain of Trp23 for interaction with MDM2 (Fig. 1). The modeling studies showed that although these compounds fit poorly into the MDM2 cleft due to steric hindrance, the spiro-(oxindole-3,3'-pyrrolidine) core structure may be used as the starting point for the design of a new class of MDM2 inhibitors. The oxindole can closely mimic the Trp23 side chain in p53 in both hydrogen bond formation and hydrophobic interactions with MDM2, and the spiropyrrolidine ring provides a rigid scaffold from which two hydrophobic groups can be projected to mimic the side chain of Phe19 and Leu26.

The series of compounds (MI-188 and others) designed by Wang's group[11] (Fig. 1) closely mimics p53 in its interaction with MDM2 and they should have a high affinity for MDM2. By now, several new small-molecule inhibitors such as RG7112 (Roche), MI-773 (Sanofi), and DS-3032b (Daiichi Sankyo) have been developed, which are at various stages of phase I clinical trials.[5]

Previously reported small-molecule inhibitors based on spiroindolinones have IC_{50} in the range 24.1 nM – 181 μM.[12] Presumably, introduction of two spiro rings in the inhibitor structure[13–15] may increase the conformational rigidity of the molecule and, as the result, improve its interaction with MDM2 protein. Based on single examples of the dispiro derivatives presented in the literature, they inhibit the p53–MDM2 interaction with IC_{50} values in the range of 0.001–0.05 μM (GI_{50} <0.1 mM in the MTT test).[16–18]

In this work, we synthesized a series of novel dispirohydantoin-based oxindoles as potential p53–MDM2 interaction inhibitors and evaluated their biological activity. Continuing our project on the discovery of potential p53–MDM2 interaction inhibitors based on 2-thiohydantoins,[14] which are structural analogs of the nutlin-3, in the present study we report a procedure for the synthesis of their oxo analogs *via* 1,3-dipolar cycloaddition reactions of azomethine ylides with 5-arylidenehydantoins.

For the synthesis of target compounds **4a**–**m** we used two synthetic routes shown in Scheme 1. Both methods represent two-step procedures starting from 2-thiohydantoins **1a**–**m** and involve replacement of sulfur by oxygen and spirocyclization, and the order of the steps may be varied. The yields of the obtained compounds **4a**–**m** are shown in Table 1.

In the first synthetic approach (method I, Scheme 1), a series of dispiroindolinones **4a**–**m** were obtained from the corresponding thiohydantoins **1a**–**m** using the procedure analogous to the earlier described protocol.[14] The first step is the nucleophilic substitution of sulfur with oxygen in thiohydantoins **1a**–**m**, achieved by two consecutive reactions – *S*-alkylation with MeI followed by hydrolysis in refluxing aqueous HCl–EtOH mixture. The presence of hydantoin moiety in the resulting products **2a**–**e**,**g**–**i**,**k**,**m** was confirmed by ^{1}H NMR spectroscopy. In all cases, ^{1}H NMR spectra of the synthesized hydantoins **2a**–**e**, **g**–**i**,**k**,**m** contained signals at 11.00–12.65 ppm, which are characteristic for NH protons in 2-arylidenehydantoins. An alternative previously described procedure, which involves treatment with chloroacetic acid in H_2O[19] for replacing sulfur with oxygen, was not successful in our case. None of the desired products were detected in reaction mixtures by LC-MS analysis. At the second step, hydantoins **2a**–**e**,**g**–**i**,**k**,**m** reacted with sarcosine and isatin in refluxing EtOH forming target dispiroindolinones **4a**–**e**,**g**–**i**,**k**,**m** in 4–8 h. This reaction occurs according to the 1,3-dipolar cycloaddition mechanism. [3+2] Cycloaddition reactions are convenient and widely used for the synthesis of five-membered heterocycles containing one to three heteroatoms.[20]

For the synthesis of bromo-substituted dispiroindolinones **4f**,**j**,**l**, we successfully used an alternative synthetic sequence (method II, Scheme 1). Initially, spiro derivatives of 2-arylidenethiohydantoins **3f**,**j**,**l**[21,22] were prepared, and then they were *S*-alkylated and hydrolyzed to yield desired 2-arylidenehydantoin dispiro compounds **4f**,**j**,**l**.

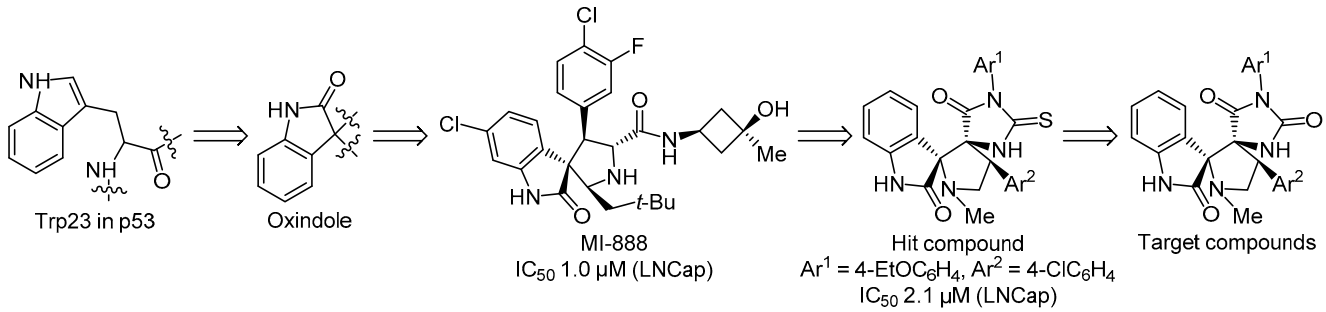

Figure 1. The logical transition from tryptophan to oxindole fragment and further to the compounds of the MI series and the compounds studied in this work (IC_{50} values are given for human prostate adenocarcinoma cell line (LNCap)).

Scheme 1. Synthesis of target dispirooxindoles **4a**–**m**

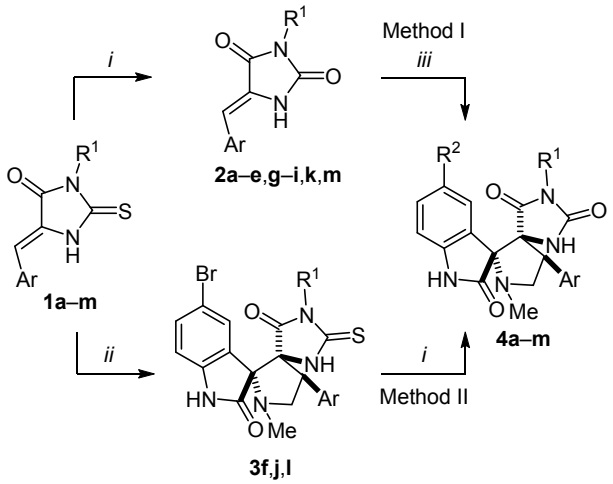

i: 1. MeI, 2% KOH in EtOH, rt, 0.5 h; 2. EtOH–HCl (1:1), Δ, 6 h
ii: 5-Bromoisatin, sarcosine, EtOH, Δ, 6 h
iii: Isatin, sarcosine, EtOH, Δ, 8 h

Table 1. Yields of target dispirooxindoles **4a**–**m**

Compound	R^1	R^2	Ar	Method	Yield, %
4a	H	H	4-ClC_6H_4	I	56
4b	Ph	H	Ph	I	68
4c	Ph	H	2-BrC_6H_4	I	93
4d	Ph	H	2-ClC_6H_4	I	97
4e	Ph	H	4-FC_6H_4	I	78
4f	Ph	Br	4-BrC_6H_4	II	72
4g	4-ClC_6H_4	H	Ph	I	75
4h	4-ClC_6H_4	H	4-$MeOC_6H_4$	I	82
4i	4-$MeOC_6H_4$	H	4-ClC_6H_4	I	39
4j	4-$EtOC_6H_4$	Br	4-ClC_6H_4	II	56
4k	3-Cl-4-FC_6H_3	H	4-$EtOC_6H_4$	I	43
4l	3-Cl-4-FC_6H_3	Br	4-ClC_6H_4	II	51
4m	3-Cl-4-FC_6H_3	H	4-$MeOC_6H_4$	I	86

The mechanism of spirocyclization reactions is presumably similar to that for the addition of azomethine ylides to *N*-substituted 5-arylidenethiohydantoins[15] and 1,3-oxazolones.[13] It involves successive reactions of isatin or 5-bromoisatin with sarcosine to form an iminium intermediate and then a lactone which loses the CO_2 molecule to afford dipole (Scheme 2). This dipole regio- and diastereoselectively attacks the C=C double bond of 5-arylidenehydantoin. Note that the attack of dipole can proceed from both above and below of the double bond plane to result in a mixture of enantiomers. Possible ways of azomethine ylide approach to dipolarophile moiety are shown in Scheme 2.

Based on the structure of the products, we can conclude that cycloaddition reaction takes place through the *exo*-transition state (Scheme 2), possibly due to an increase in the transition state energy as a result of electrostatic repulsion of the *cis*-located carbonyl groups of azomethine ylide and dipolarophile in other approaches.[23,24] Thus, *exo* approach of azomethine ylide to dipolarophile C=C double bond is realized.

The structures of compounds **4a**–**m** were established based on ^1H and ^{13}C NMR spectroscopy and mass spectrometry data. For all products, ^1H NMR spectra showed the signals of indolinone NH protons at 10.60–10.85 ppm, NH protons of 2-arylidenehydantoin moiety at 8.02–8.64 ppm, aromatic protons as multiplets at 6.85–7.96 ppm, characteristic pseudo-triplets of three CH protons of pyrrolidine cycles at 4.09–4.61, 3.79–4.20, and 3.37–3.46 ppm, as well as the signal of NCH_3 protons at 2.08–2.19 ppm. ESI HRMS spectra of compounds **4a**–**m** confirmed the composition of the synthesized products. Notably, all dispiro derivatives were isolated from reaction mixtures as single diastereomers with (2'*R**,4*S**,4'*S**) relative configurations.

For compound **4d**, COSY, NOESY, and ^1H–^{13}C HSQC spectra were recorded (Supplementary information file). In the ^1H NMR spectrum of compound **4d**, there are three signals of the pyrrolidine cycle protons at 4.61, 4.20, and 3.43 ppm as characteristic pseudo-triplets (Supplementary information file, Fig. S26). In the COSY spectrum of compound **4d**, the cross peaks are observed, indicating pairwise interaction of protons at 4.61, 4.20, 3.43 ppm with each other with the similar coupling constants (Supplementary information file, Fig. S27). For determination of the relative position of protons and carbon atoms, ^1H–^{13}C HSQC correlation spectroscopy was used (Supplementary information file, Fig. S28). As this experiment demonstrates, for the proton with a chemical shift of 4.61 ppm, cross peak with the carbon atom at 44.8 ppm is observed, and for the proton at 4.20 and 3.43 ppm, cross peak with the carbon of 55.5 ppm is also observed. Thus, proton at 4.61 ppm is located at position 4 of the pyrrolidine cycle, and the other two protons are at position 5 of the cycle. To see an interaction of the protons at position 5 of pyrrolidine cycle with the sides of the diastereotope surface, NOESY NMR spectroscopy was used (Supplementary information file, Figs. S29–S31). When the proton at 3.43 ppm was irradiated at its resonant frequency, the responses of the NH protons of thiohydantoin cycle and indole fragment were observed (Supplementary information file, Fig. S29). Therefore, these protons are located from the same side of the pyrrolidine cycle plane. The other two protons of the pyrrolidine fragment have a weak correlation with each other (Supplementary information file, Fig. S28, S29), which means they are located on the same side of the central cycle of the molecule. Thereby, the proton at 3.43 ppm is located on the opposite side of the cycle from protons at 4.20 and 4.61 ppm, which differ greatly among themselves according to ^1H–^{13}C HSQC. Thus, using the methods of one-dimensional and two-dimensional NMR spectroscopy, it was possible to establish the assignment of protons to their signals in the NMR spectrum, as well as to prove the stereochemical structure of the obtained compound.

Molecular structure of compound **4l** was also confirmed by X-ray crystallography (Supplementary information file, Fig. 2, Table S1), which showed the formation of the diastereomer with (2'*R**,4*S**,4'*S**) relative configuration.

Scheme 2. Possible approaches of azomethine ylide dipole to 5-arylidenehydantoin in the 1,3-dipolar cycloaddition reactions leading to the possible formation of various diastereomeric products (the actual reaction pathway is shown in blue)

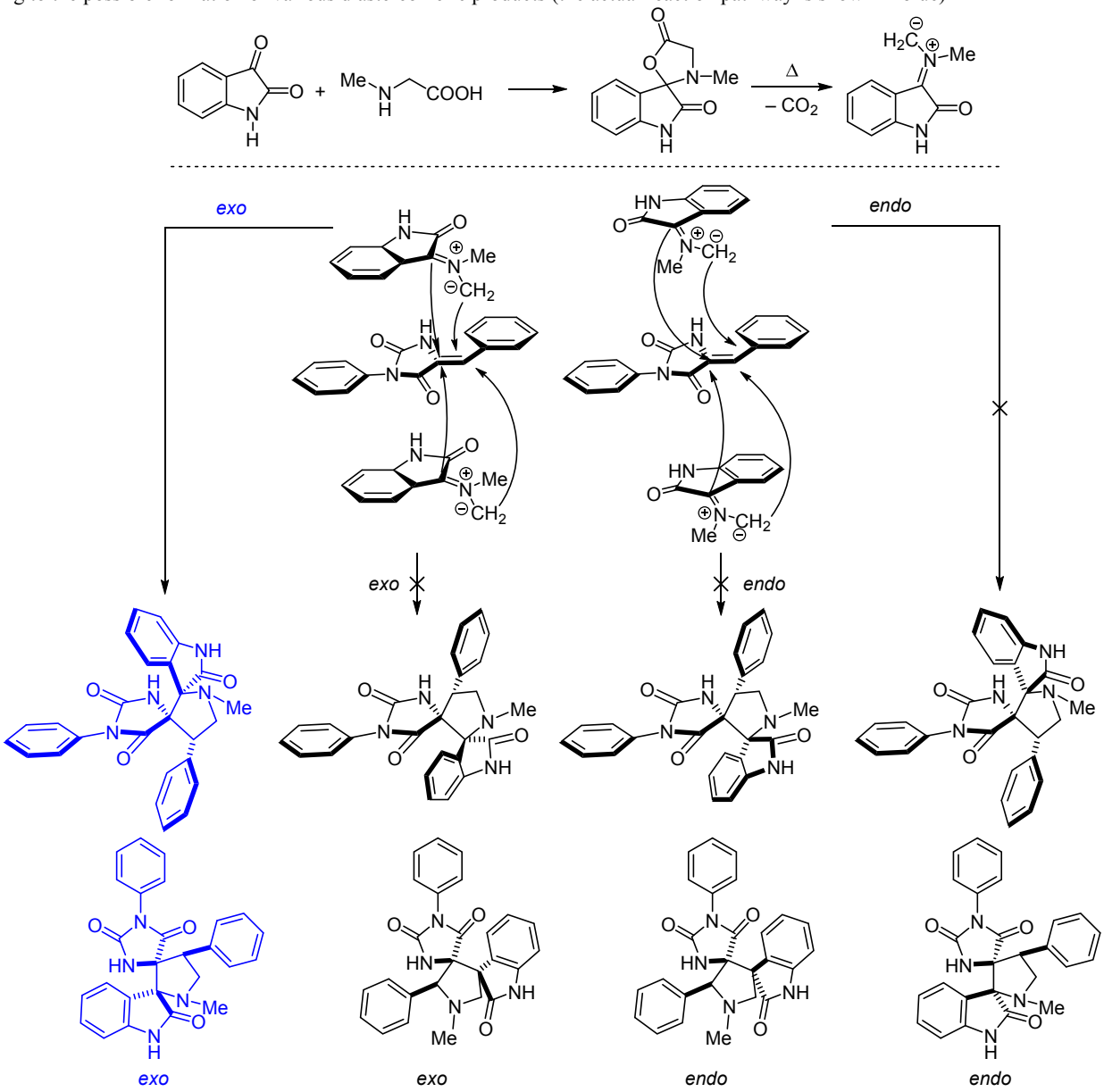

The neighboring spiro-conjugated cycles are almost planar and near perpendicular to each other. The unit cell in the crystal of compound **4l** contains two enantiomeric molecules in *P*1 space group with the inversion center.

When 5-bromoisatin was used instead of unsubstituted isatin in [3+2] cycloadditions with 5-arylidenehydantoins **2a**–**e**,**g**–**i**,**k**,**m** ($R^2 \neq H$), we could not obtain the desired dispiro products, and only starting materials were isolated from the reaction mixtures. This result can be rationalized by steric hindrances between 1,3-dipole and *N*-substituted arylidenehydantoin arising in the transition state that would lead to product formation (Scheme 3). In this case, isatin bromine atom in the transition state should be located close to R^1 substituent at the N(3) atom of hydantoin, not allowing the reagents to approach each other. The significance of steric bulk introduced by R^1 group is supported by the fact that the plane of benzene ring of R^1 in hydantoin molecules

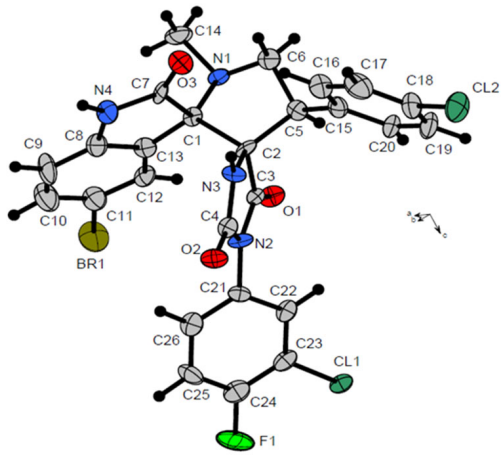

Figure 2. Molecular structure of compound **4l** with atoms represented as thermal vibration ellipsoids of 40% probability.

Scheme 3. Steric hindrances arising upon the convergence of the 1,3-dipole and *N*-substituted arylidenehydantoin

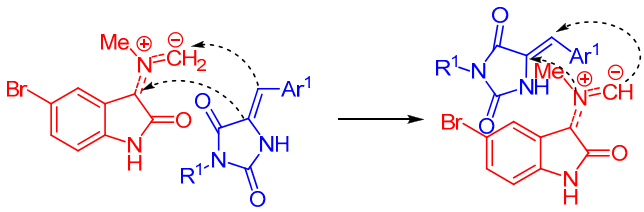

is almost perpendicular to the plane of the imidazolone ring (as we reported earlier[25] and Scheme 3).

In this case, for the synthesis of bromo-substituted dispiroindolinones **4f**,**j**,**l**, we have successfully used an alternative synthetic method II (Scheme 1).

Thus, two alternative methods for the preparation of the target dispiroindolinones **4a**–**m**, differing in the sequence of the stages of cycloaddition and replacement of the *exo*-cyclic sulfur atom with oxygen have been developed. In general, method I with the initial preparation of hydantoin and its further introduction into spirocyclization seems to be more convenient, allowing purification of products by recrystallization at all stages of the synthesis. However, this method is not applicable using 5-bromoisatin, and in this case, the use of the method II with the initial spirocyclization and the further replacement of the thio-hydantoin fragment sulfur with oxygen may be rational, although, the intermediate dispirothiohydantoin sometimes requires purification by column chromatography.

Considering the literature data[18] we proposed that stability and pharmacokinetic profile of dispiro derivatives based on 5-arylidenehydantoins would be enhanced in comparison to their thiohydantoin analogs. On the basis of the molecular docking data, 2-oxotetrahydro-4*H*-imidazol-4-one derivatives could be effective inhibitors of the p53–MDM2 protein–protein interaction.

More than 50 crystallographic complexes obtained for various small-molecule p53–MDM2 inhibitors, including spiroindolinones, are available from PDB (Protein Data Bank). To elucidate the possible binding affinity of the target compounds toward MDM2, a static 3D molecular docking study was performed using the ICM-Pro software based on X-ray analysis data, including compounds 4HG7 (nutlin-3a) and 4JVR, a compound structurally similar to those investigated in this paper, as known p53 ligand (Fig. 3).

Water molecules were removed from the site, and the reference compounds were docked into the constructed model starting from 2D structures. The obtained results correlate with the X-ray data (Fig. 4A,B). Compounds **4l** and **4i** were then docked into the static pocket using an extensive range of key force fields, particularly describing hydrophobic interactions (Fig. 4B,C). Compounds **4l** and **4i** were compared with previously described thiohydantoin analogs **3l** and **3i**;[14] an extra docking procedure for the similar oxo and thio derivatives was performed and analyzed.

First of all, it could be noted, that key interactions of hydantoins **4l** and **4i** with MDM2 pocket (Fig. 4B,C) are the same as presented in X-ray data for reference ligand in

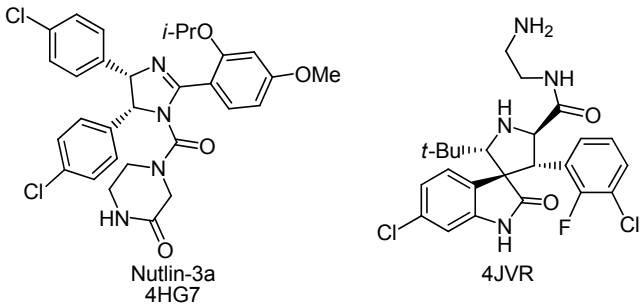

Figure 3. Nutlin-3a and compound 4JVR.

4JVR protein (Fig. 4A), namely: (a) hydrogen bond between 2-indolinone fragment and Leu54 amide carbonyl group; (b) hydrogen bond between 2-oxo group of hydantoin scaffold and His96 along with π-stacking between ligand ring and His96 residue. Secondly, the score functions of thio derivatives **3l** and **3i** demonstrated that their binding to the active site is slightly less preferable than for oxo analogs. Moreover, it should be noted that the binding mode of hydantoins **4l** and **4i** significantly differs from that of the thio analogs and does not well correlate with reference data (Fig. 4D–F): during the docking procedure, no key interactions were observed. This fact could be explained by the larger size of the sulfur atom in thiohydantoin moiety in contrast with the oxygen atom in hydantoin analog, which makes difficult for thiohydantoins **3l** and **3i** to entry in the hydrophobic pocket of MDM2 and interact with His96. In all orientations, the sulfur atom of compounds **3l** and **3i** is positioned "out-of-pocket" (Fig. 4D), while orientations performed for oxo derivatives **4l** and **4i** showed "in-pocket" positioning for both oxygen atoms. The repulsion of sulfur atom from MDM2 binding mode seemed to be crucial for the "right" orientation that we can observe in 4JVR X-ray diffraction data. Thus, according to molecular

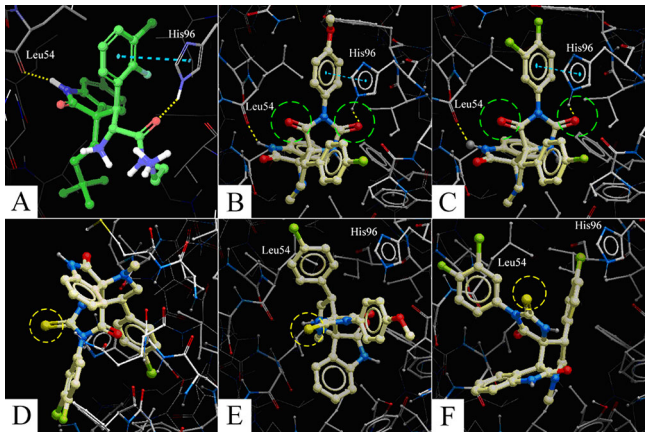

Figure 4. Molecular docking of 4JVR ligand and compounds **3i**,**l** and **4i**,**l** into hydrophobic MDM2 binding pocket. (A) 3D structure of 4JVR (X-ray data) in hydrophobic MDM2 binding pocket[10] (yellow dashed line – H bond; blue dashed line – π-stacking; green dashed circle – "in-pocket" positioning; yellow dashed circle – "out-of-pocket" positioning); (B) The orientation of compound **4i**; (C) The orientation of compound **4l**; (D) The orientation of compound **3l** with "out-of-pocket" conformation of 2-sulfur atom; (E) The orientation of compound **3i**; (F) The orientation of compound **3l**.

docking study, dispiroindolinones based on hydantoin core should have better binding affinity to MDM2.

Further, the cytotoxicity of the synthesized dispiroindolinones **4a**–**m** on the selected model cell lines was investigated. This study was realized using breast cancer MCF7, human lung carcinoma A549, human embryonic kidney HEK293T, and lung fibroblast VA13 cell lines. Cytotoxicity of the tested compounds was assessed using the MTT (3-(4,5-dimethylthiazol-2-yl)-2,5-diphenyltetrazolium bromide) assay,[26] all compounds were additionally tested for the p53 activation on a transcriptional reporter.[27, 28] The results of these assays are shown in Table 2, along with the results obtained for nutlin-3 as known inhibitor of p53–MDM2 interaction and cisplatin as a cytotoxic drug that does not act by the p53–MDM2 inhibition mechanism.

The most cytotoxic compound **4l** demonstrates high cytotoxicity with IC_{50} value in the range of 1.3–4.7 μM against all cell lines (Table 2). However, no relevant selectivity was observed for the most active compounds among the cell types. Four compounds **4e**,**i**,**j**,**l** showed moderate selectivity against A549 cell line with IC_{50} value in the range of 1.3–7.5 μM. It should be noted that hydantoins **4j**–**l** showed higher cytotoxicity against HEK293T and MCF7 cell lines compared to corresponding thio analogs.[14] For example, compound **4j** has IC_{50} equal to 6.3 ± 0.6 μM at HEK293T cell line and IC_{50} equal to 6.6 ± 0.6 μM at MCF7 cell line, while its thio analog **3j** has IC_{50} equal to 28.61 ± 8.68 μM and 34.9 ± 6.4 μM, respectively.[14] Compound **4l** has IC_{50} equal to 3.0 ± 0.1 μM at HEK293T cell line and IC_{50} equal to 3.9 ± 0.3 μM at MCF7 cell line, whereas its thio analog **3l** has IC_{50} equal to 15.62 ± 3.34 μM and 15.52 ± 2.31 μM, respectively.[14]

The synthesized compounds were also tested for activation of p53 in transcriptional reporter activation test[28] (Table 2). Nutlin, a known inhibitor of p53–MDM2 interaction was used as a positive control. We proceeded from the assumption that the mechanisms of the cytotoxicity of the studied compounds may include the p53 activation. It is known that the activated p53 induces the transcription of MDM2, which can directly interact with transactivation domain of p53, thereby inhibiting its transcription activity by targeting it for polyubiquitination and further proteasome-mediated degradation.[29] In many cancer cells lines, including HEK293T, MCF7, and A549, the overexpression of MDM2 is actually observed, resulting in significant apoptosis attenuation.[14] Nutlin-3a causes direct activation of p53 *via* the block of p53–MDM2 interaction and elevates p53 activity up to five times in the reporter assay.[6] Treatment of the cells with cisplatin causes DNA damage that leads to p53 activation indirectly due to regulatory cascades: it causes about twofold p53 activation in the reporter-based experiments.[30] In our case, two compounds **4j**,**l** showed higher *in vitro* cytotoxicity against MCF7 and A549 cell lines compared with nutlin-3a and cisplatin. The treatment of the cells with compounds **4a**,**g** leads to the twofold p53 activation; it is less than for nutlin-3a, but comparable with indirect cisplatin action, which suggests that the investigated compounds have indirect p53-dependent mechanism of action.[6]

Table 2. Cytotoxicity (IC_{50}, μM) and p53 reporter activation test for the synthesized compounds **4a**–**m** against different cancer cell lines

Compound	Cancer cell lines				p53 reporter activation test
	MCF7	A549	HEK293T	VA13	
4a	19.3 ± 1.4	21.0 ± 1.4	12.6 ± 1.3	24.3 ± 2.0	2.5
4b	≥100	88.6 ± 9.4	23.6 ± 1.2	≥100	na*
4c	47.3 ± 3.3	39.6 ± 2.3	28.8 ± 6.2	54.2 ± 4.8	na
4d	70.1 ± 5.9	55.1 ± 4.5	35.4 ± 2.3	≥100	1.7
4e	24.1 ± 4.1	6.6 ± 1.6	9.2 ± 0.5	11.9 ± 2.5	na
4f	≥100	≥100	≥100	≥100	na
4g	20.0 ± 2.3	14.1 ± 1.2	15.8 ± 1.2	47.3 ± 4.6	2.3
4h	≥100	≥100	≥100	≥100	na
4i	18.4 ± 5.3	7.5 ± 2.0	14.3 ± 5.0	20.8 ± 5.3	na
4j	6.6 ± 0.6	4.9 ± 0.3	6.3 ± 0.6	13.3 ± 0.8	na
4k	7.7 ± 0.6	11.9 ± 0.8	8.1 ± 0.6	16.2 ± 1.6	1.7
4l	3.9 ± 0.3	1.3 ± 0.1	3.0 ± 0.1	4.7 ± 0.3	1.6
4m	58.2 ± 12.8	41.8 ± 6.4	35.9 ± 2.6	33.5 ± 2.7	na
Nutlin-3[22]	14.9 ± 0.6	10.4 ± 0.8	N/A**	N/A	6.9
Cisplatin	7.1 ± 0.8	4.1 ± 0.6	4.3 ± 0.9	2.2 ± 0.3	2.1

* na – not active compound.
** N/A – not applicable.

In general, we assume that the observed data of biological activity could be rationalized in two ways. High cytotoxicity of compounds **4j**,**l** with simultaneous absence of p53 activation effect may be the result of two parallel effects: the activation of p53 and other mechanisms that affects the general cytotoxicity. The second possible explanation is that weak p53 activation is a consequence of other types of activities that cause p53 expression. Thus, a high cytotoxicity, but the absence of p53 activation for compounds **4j**,**l** is more a consequence of the general toxic effect of the molecule by a p53-independent mechanism than the competitive processes of p53 activation. Apparently, p53 protein is not the only target of the cytotoxic effect of the compounds obtained. Although according to the results of molecular docking they are capable of fitting into the pocket of MDM2, they obviously do not possess the ability of direct p53 activation, like nutlin. However, the resulting hydantoin-based dispiroindolinones have higher toxicity than previously obtained oxazolone analogs,[13] and some ability to activate p53, which was not observed at all for thiohydantoin analogs.[14]

In summary, a series of novel dispiroindolinones based on 2-arylidenehydantoins were synthesized starting from 5-arylmethylene-2-hydantoins, isatins, and sarcosine using two alternative methods. Some of the obtained dispiroindolinones exhibit moderate anticancer activity against A549 cell lines in micromolar concentrations. Two dispiroindolinones show moderate p53 activation in p53 reporter activation test. Cytotoxicity of the obtained dispiroindolinones based on 5-arylmethylene-2-hydantoins is higher than the cytotoxicity of its previously studied thio analogs.

Experimental

^{1}H and ^{13}C NMR spectra and 2D NMR experiments were recorded on a Bruker Avance 400 spectrometer (400 and 100 MHz, respectively) in DMSO-d_6, TMS was used as internal standard. High-resolution mass spectra were recorded on an Orbitrap Elite mass spectrometer (ESI). Melting points were measured on a Stuart melting point apparatus SMP11 in open capillaries and are uncorrected. TLC analysis was carried out on silica gel plates Silufol UV254.

All reagents and solvents were reagent grade or were purified by standard methods before use. Compounds **1a**–**m**,[25] **2a**–**c**,**e**–**f**,**h**,[31] **3j,l** [14] were prepared according to the previously reported procedures. The synthesis of compounds **2b**,**g**,**i**–**l**[31] and **3f**,**i**,**k**[14] was carried out analogously to the previously reported procedures (described in Supplementary information file).

Synthesis of compounds 4a–m (General procedure). Method I. Sarcosine (2 mmol) and isatin (2 mmol) were added to a stirred and refluxed solution of the respective compound **2a**–**e**,**g**–**i**,**k**,**m** (1 mmol) in EtOH (10 ml). The resulted solution was refluxed for 8 h. After cooling to room temperature, formed precipitate was filtered off and washed with EtOH.

Method II. MeI (1 equiv) was added to a solution of compound **3f**,**j**,**l** (1 equiv) in 2% KOH in EtOH (10 ml), and the reaction mixture was stirred at room temperature for 30 min. The precipitate formed was filtered off and dried on air. Then the resulting salt was dissolved in EtOH–HCl, 1:1 mixture (10 ml) and refluxed for 6 h. After cooling, the precipitate was filtered off and dried on air.

4'-(4-Chlorophenyl)-1'-methyldispiro[imidazolidine-4,3'-pyrrolidine-2',3''-indoline]-2,2'',5-trione (4a). Yield 222 mg (56%, method I), white solid, mp 216–218°C. ^{1}H NMR spectrum, δ, ppm (*J*, Hz): 11.72 (1H, s, NH indolinone); 10.68 (1H, s, NH imidazolidine); 9.74 (1H, s, H Ar); 7.52 (1H, s, H Ar); 7.45 (1H, d, *J* = 7.7, H Ar); 7.41–7.36 (4H, m, H Ar); 6.77 (1H, d, *J* = 7.7, H Ar); 4.16 (1H, t, *J* = 9.5, H pyrrolidine); 3.81 (1H, t, *J* = 9.5, H pyrrolidine); 3.41 (1H, t, *J* = 8.9, H pyrrolidine); 2.10 (3H, s, CH_3). ^{13}C NMR spectrum, δ, ppm: 176.9; 172.0; 157.0; 144.1; 135.1; 132.1; 131.4; 130.3; 128.6; 126.2; 125.8; 125.0; 122.3; 110.2; 107.3; 76.8; 54.3; 45.3; 36.2; 26.4. Found, *m*/*z*: 397.0991 $[M+H]^+$. $C_{20}H_{18}ClN_4O_3$. Calculated, *m*/*z*: 397.1062.

1'-Methyl-1,4'-diphenyldispiro[imidazolidine-4,3'-pyrrolidine-2',3''-indoline]-2,2'',5-trione (4b). Yield 298 mg (68%, method I), white solid, mp 221–223°C. ^{1}H NMR spectrum, δ, ppm (*J*, Hz): 10.62 (1H, s, NH indolinone); 8.14 (1H, s, NH imidazolidine); 7.96 (1H, d, *J* = 7.9, H Ar); 7.39–7.27 (9H, m, H Ar); 7.03 (1H, t, *J* = 7.2, H Ar); 6.84 (1H, d, *J* = 8.2, H Ar); 6.80 (2H, d, *J* = 7.0, H Ar); 4.25 (1H, t, *J* = 9.5, H pyrrolidine); 3.98 (1H, t, *J* = 9.5, H pyrrolidine); 3.43 (1H, t, *J* = 9.1, H pyrrolidine); 2.14 (3H, s, CH_3). ^{13}C NMR spectrum, δ, ppm: 175.7; 172.6; 153.7; 143.4; 135.8; 131.3; 130.0; 129.8; 128.9; 128.6; 128.1; 127.4; 127.0; 126.3; 124.3; 121.6; 109.8; 77.4; 74.5; 66.4; 57.2; 50.1; 34.7. Found, *m*/*z*: 439.1757 $[M+H]^+$. $C_{26}H_{23}N_4O_3$. Calculated, *m*/*z*: 438.1765.

4'-(2-Bromophenyl)-1'-methyl-1-phenyldispiro[imidazolidine-4,3'-pyrrolidine-2',3''-indoline]-2,2'',5-trione (4c). Yield 480 mg (93%, method I), white solid, mp 206–208°C. ^{1}H NMR spectrum, δ, ppm (*J*, Hz): 10.60 (1H, s, NH indolinone); 8.02 (1H, s, NH imidazolidine); 7.64 (1H, d, *J* = 7.5, H Ar); 7.51–7.27 (9H, m, H Ar); 7.03 (1H, t, *J* = 8.0, H Ar); 6.85 (2H, d, *J* = 7.5, H Ar); 4.61 (1H, t, *J* = 8.7, H pyrrolidine); 4.13 (1H, t, *J* = 8.7, H pyrrolidine); 3.46 (1H, t, *J* = 8.1, H pyrrolidine); 2.14 (3H, s, CH_3). ^{13}C NMR spectrum, ppm: 175.8; 173.1; 163.1; 154.2; 144.0; 135.6; 133.0; 132.4; 131.9; 130.4; 130.3; 129.3; 128.9; 128.1; 126.9; 126.4; 124.1; 123.7; 121.8; 110.0; 107.2; 77.0; 73.5; 56.4; 47.3; 34.8. Found, *m*/*z*: 517.0877 $[M+H]^+$. $C_{26}H_{22}BrN_4O_3$. Calculated, *m*/*z*: 517.0870.

4'-(2-Chlorophenyl)-1'-methyl-1-phenyldispiro[imidazolidine-4,3'-pyrrolidine-2',3''-indoline]-2,2'',5-trione (4d). Yield 458 mg (97%, method I), white solid, mp 225–227°C. ^{1}H NMR spectrum, δ, ppm (*J*, Hz): 10.63 (1H, s, NH indolinone); 8.15 (1H, s, NH imidazolidine); 7.96 (1H, d, *J* = 7.5, H Ar); 7.49–7.27 (9H, m, H Ar); 7.04 (1H, t, *J* = 7.5, H Ar); 6.88–6.81 (1H, m, H Ar); 4.62 (1H, t, *J* = 9.0, H pyrrolidine); 4.20 (1H, t, *J* = 9.0, H pyrrolidine); 3.44 (1H, t, *J* = 8.5, H pyrrolidine); 2.15 (3H, s, CH_3). ^{13}C NMR spectrum, δ, ppm: 175.8; 173.3; 154.2; 144.0; 134.8; 133.8; 131.5; 131.3; 130.3; 129.1; 129.0; 128.9 (2C); 128.1; 127.6; 126.9; 126.5; 126.3; 123.7; 121.8; 109.9; 77.0; 73.5; 55.5; 44.8; 34.8. Found, *m*/*z*: 473.1375 $[M+H]^+$. $C_{26}H_{22}ClN_4O_3$. Calculated, *m*/*z*: 473.1375.

4'-(4-Fluorophenyl)-1'-methyl-1-phenyldispiro[imidazolidine-4,3'-pyrrolidine-2',3''-indoline]-2,2'',5-trione (4e). Yield 355 mg (78%, method I), white solid, mp 232–234°C. ^{1}H NMR spectrum, δ, ppm (*J*, Hz): 10.61 (1H, s, NH indolinone); 8.43 (1H, s, NH imidazolidine); 7.46 (2H, t, *J* = 9.5, H Ar); 7.37 (2H, d, *J* = 8.3, H Ar); 7.29 (2H, t, *J* = 8.3, H Ar); 7.05–6.99 (2H, m, H Ar); 6.91–6.83 (5H, m, H Ar); 4.20 (1H, t, *J* = 8.7, H pyrrolidine); 3.91 (1H, t, *J* = 8.7, H pyrrolidine); 3.40 (1H, t, *J* = 7.9, H pyrrolidine); 2.12 (3H, s, CH_3). ^{13}C NMR spectrum, δ, ppm: 176.3; 169.5; 159.1; 155.4; 144.2; 131.5; 130.2; 129.3; 128.5; 127.0; 126.7; 126.2; 122.2; 114.1; 110.5; 76.3; 76.0; 74.8; 55.5; 55.4; 54.5; 49.8; 45.4; 36.5; 35.2; 26.5. Found, *m*/*z*: 456.1596 $[M+H]^+$. $C_{26}H_{22}FN_4O_3$. Calculated, *m*/*z*: 456.1598.

5''-Bromo-4'-(4-bromophenyl)-1'-methyl-1-phenyldispiro[imidazolidine-4,3'-pyrrolidine-2',3''-indoline]-2,2'',5-trione (4f). Yield 410 mg (72%, method II), white solid, mp 251–253°C. ^{1}H NMR spectrum, δ, ppm (*J*, Hz): 10.87 (1H, s, H indolinone); 9.05 (1H, s, H imidazolidine); 7.50 (1H, dd, ^1J= 8.2, ^2J= 2.0, H Ar); 7.42 (4H, br. s, H Ar); 7.25 (1H, d, *J* = 2.0, H Ar); 6.88–6.83 (4H, m, H Ar); 6.37 (1H, s, H Ar); 6.34 (1H, s, H Ar); 3.98 (1H, t, *J* = 6.9, H pyrrolidine); 3.89 (1H, t, *J* = 8.9, H pyrrolidine); 3.44 (1H, t, *J* = 9.2, H pyrrolidine); 2.18 (3H, s, CH_3). ^{13}C NMR spectrum, δ, ppm: 175.1; 172.5; 153.6; 142.7; 135.0; 132.8; 132.2; 131.4; 131.2; 129.4; 128.9; 128.3; 126.6; 126.3; 120.8; 113.5; 111.9; 98.4; 77.3; 74.4; 57.1; 49.2; 34.8. Found, *m*/*z*: 593.9904 $[M+H]^+$. $C_{26}H_{21}Br_2N_4O_3$. Calculated, *m*/*z*: 593.9902.

1-(4-Chlorophenyl)-1'-methyl-4'-phenyldispiro[imidazolidine-4,3'-pyrrolidine-2',3''-indoline]-2,2'',5-trione

(4g). Yield 355 mg (75%, method I), white solid, mp 211–213°C. ^{1}H NMR spectrum, δ, ppm (*J*, Hz): 10.62 (1H, s, NH indolinone); 8.41 (1H, s, NH imidazolidine); 7.70 (2H, d, *J* = 7.2, H Ar); 7.55 (2H, d, *J* = 7.2, H Ar); 7.25–7.19 (5H, m, H Ar); 7.09–6.85 (4H, m, H Ar); 4.25 (1H, t, *J* = 8.7, H pyrrolidine); 3.97 (1H, t, *J* = 8.7, H pyrrolidine); 3.43 (1H, t, *J* = 9.3, H pyrrolidine); 2.13 (3H, s, CH_3). ^{13}C NMR spectrum, δ, ppm: 175.6; 172.3; 153.2; 143.4; 135.6; 132.5; 130.1; 130.0; 129.8; 129.0; 128.6; 128.5; 127.8; 127.4; 126.8; 124.2; 121.6; 120.4; 109.8; 77.4; 74.5; 57.1; 50.0; 34.7. Found, *m*/*z*: 472.1304 $[M+H]^+$. $C_{26}H_{22}ClN_4O_3$. Calculated, *m*/*z*: 472.1302.

1-(4-Chlorophenyl)-4'-(4-methoxyphenyl)-1'-methyldispiro[imidazolidine-4,3'-pyrrolidine-2',3''-indoline]-2,2'',5-trione (4h). Yield 412 mg (82%, method I), white solid, mp 236–238°C. ^{1}H NMR spectrum, δ, ppm (*J*, Hz): 10.64 (1H, s, NH indolinone); 8.35 (1H, s, NH imidazolidine); 7.49 (2H, d, *J* = 7.4, H Ar); 7.39–7.31 (4H, m, H Ar); 7.19 (2H, d, *J* = 7.4, H Ar); 7.03 (2H, d, *J* = 7.4, H Ar); 6.85–6.80 (2H, m, H Ar); 4.25 (1H, t, *J* = 9.9, H pyrrolidine); 3.92 (1H, t, *J* = 9.9, H pyrrolidine); 3.56 (3H, s, OCH_3); 3.43 (1H, t, *J* = 8.7, H pyrrolidine); 2.12 (3H, s, CH_3). ^{13}C NMR, δ, ppm: 175.6; 172.4; 163.1; 159.7; 158.5; 153.8; 143.3; 132.3; 131.4; 130.9; 128.8; 128.5; 127.8; 125.3; 124.3; 124.2; 114.4; 113.9; 110.7; 74.5; 55.3; 55.0; 34.7. Found, *m*/*z*: 503.1481 $[M+H]^+$. $C_{27}H_{24}ClN_4O_4$. Calculated, *m*/*z*: 503.1481.

4'-(4-Chlorophenyl)-1-(4-methoxyphenyl)-1'-methyldispiro[imidazolidine-4,3'-pyrrolidine-2',3''-indoline]-2,2'',5-trione (4i). Yield 196 mg (39%, method I), white solid, mp 227–229°C. ^{1}H NMR spectrum, δ, ppm (*J*, Hz): 10.59 (1H, s, NH indolinone); 8.22 (1H, s, NH imidazolidine); 7.31–7.23 (8H, m, H Ar); 7.04–6.82 (2H, m, H Ar); 6.65 (2H, d, *J* = 9.0, H Ar); 4.19 (1H, t, *J* = 9.4, H pyrrolidine); 3.89 (1H, t, *J* = 9.4, H pyrrolidine); 3.88 (3H, s, OCH_3); 3.39 (1H, t, *J* = 8.2, H pyrrolidine); 2.08 (3H, s, CH_3). ^{13}C NMR spectrum, δ, ppm: 169.6; 159.4; 155.5; 145.5; 144.1; 133.9; 133.0; 131.4; 130.8; 129.0; 128.7; 127.8; 126.3; 125.8; 123.5; 123.2; 114.7; 114.6; 109.7; 76.0; 75.6; 75.5; 55.8; 54.3; 45.5; 36.7; 35.1. Found, *m*/*z*: 503.1481 $[M+H]^+$. $C_{27}H_{24}ClN_4O_4$. Calculated, *m*/*z*: 503.1481.

5''-Bromo-4'-(4-chlorophenyl)-1-(4-ethoxyphenyl)-1'-methyldispiro[imidazolidine-4,3'-pyrrolidine-2',3''-indoline]-2,2'',5-trione (4j). Yield 289 mg (56%, method II), white solid, mp 247–259°C. ^{1}H NMR spectrum, δ, ppm (*J*, Hz): 10.91 (1H, s, H indolinone); 9.14 (1H, s, H imidazolidine); 7.57–7.32 (2H, m, H Ar); 7.50 (1H, d, *J* = 7.1, H Ar); 7.45–7.30 (5H, m, H Ar); 7.27 (1H, s, H Ar); 6.87–6.85 (1H, m, H Ar); 6.50 (2H, d, *J* = 7.1, H Ar); 4.60 (2H, t, *J* = 9.0, OCH_2); 3.90 (1H, t, *J* = 8.4, H pyrrolidine); 3.86 (1H, t, *J* = 8.9, H pyrrolidine); 3.50 (1H, t, *J* = 9.1, H pyrrolidine); 2.20 (3H, s, CH_3); 1.45 (3H, s, CH_3). ^{13}C NMR spectrum, δ, ppm: 174.5; 169.2; 158.3; 155.0; 143.2; 133.5; 133.4; 130.5; 128.6; 128.3; 127.5; 127.4; 125.3; 123.5; 123.0; 114.8; 114.7; 113.7; 112.4; 75.8; 75.4; 74.3; 63.4; 54.0; 49.1; 44.7; 36.6; 26.3. Found, *m*/*z*: 595.0742 $[M+H]^+$. $C_{28}H_{25}BrClN_4O_4$. Calculated, *m*/*z*: 595.0742.

1-(3-Chloro-4-fluorophenyl)-4'-(4-ethoxyphenyl)-1'-methyldispiro[imidazolidine-4,3'-pyrrolidine-2',3''-indoline]-2,2'',5-trione (4k). Yield 230 mg (43%, method I), white solid, mp 219–221°C. ^{1}H NMR spectrum, δ, ppm (*J*, Hz): 10.75 (1H, s, NH indolinone); 8.57 (1H, s, NH imidazolidine); 7.48 (2H, d, *J* = 8.6, H Ar); 7.42 (1H, s, H Ar); 7.35 (2H, d, *J* = 8.2, H Ar); 7.21 (2H, d, *J* = 7.7, H Ar); 6.97–6.91 (2H, m, H Ar); 6.88 (2H, d, *J* = 8.2, H Ar); 4.19 (1H, t, *J* = 10.4, H pyrrolidine); 4.05–4.00 (2H, m, OCH_2); 3.87 (1H, t, *J* = 10.4, H pyrrolidine); 3.42 (1H, t, *J* = 10.4, H pyrrolidine); 2.14 (3H, s, CH_3); 1.17 (3H, t, *J* = 7.4, CH_3). ^{13}C NMR spectrum, δ, ppm: 175.3; 169.2; 158.4; 155.9; 154.5; 143.4; 134.5; 133.8; 133.1; 132.1; 130.7; 128.7; 128.1; 127.2; 125.8; 120.6; 120.4; 118.1; 114.2; 112.9; 77.6; 76.3; 76.0; 74.9; 54.1; 45.3; 36.5; 35.2. Found, *m*/*z*: 535.1543 $[M+H]^+$. $C_{28}H_{24}ClFN_4O_4$. Calculated, *m*/*z*: 535.1543.

5''-Bromo-1-(3-chloro-4-fluorophenyl)-4'-(4-chlorophenyl)-1'-methyldispiro[imidazolidine-4,3'-pyrrolidine-2',3''-indoline]-2,2'',5-trione (4l). Yield 298 mg (51%, method II), white solid, mp 263–265°C. ^{1}H NMR spectrum, δ, ppm (*J*, Hz): 10.80 (1H, s, NH indolinone); 8.64 (1H, s, NH imidazolidine); 7.72 (1H, d, *J* = 8.0, H Ar); 7.52–7.48 (4H, m, H Ar); 7.40 (2H, d, *J* = 9.3, H Ar); 7.11 (1H, d, *J* = 8.8, H Ar); 6.95 (1H, m, H Ar); 6.83 (1H, d, *J* = 8.0, H Ar); 6.65 (1H, s, H Ar); 4.23 (1H, t, *J* = 8.0, H pyrrolidine); 3.91 (1H, t, *J* = 8.0, H pyrrolidine); 3.47 (1H, t, *J* = 9.4, H pyrrolidine); 2.15 (3H, s, CH_3). Found, *m*/*z*: 602.9996 $[M+H]^+$. $C_{26}H_{19}BrCl_2FN_4O_3$. Calculated, *m*/*z*: 602.9997.

1-(3-Chloro-4-fluorophenyl)-4'-(4-methoxyphenyl)-1'-methyldispiro[imidazolidine-4,3'-pyrrolidine-2',3''-indoline]-2,2'',5-trione (4m). Yield 432 mg (86%, method I), white solid, mp 225–227°C. ^{1}H NMR spectrum, δ, ppm (*J*, Hz): 10.65 (1H, s, NH indolinone); 8.54 (1H, s, NH imidazolidine); 7.73 (1H, d, *J* = 9.6, H Ar); 7.51–7.44 (3H, m, H Ar); 7.40 (2H, d, *J* = 7.2, H Ar); 7.32–7.27 (2H, m, H Ar); 7.08 (1H, d, *J* = 7.8, H Ar); 7.01 (1H, t, *J* = 7.8, H Ar); 6.85 (1H, t, *J* = 7.8, H Ar); 4.24 (1H, t, *J* = 9.0, H pyrrolidine); 3.94 (1H, t, *J* = 9.0, pyrrolidine); 3.45 (1H, t, *J* = 7.8, H pyrrolidine); 2.12 (3H, s, CH_3). ^{13}C NMR spectrum, δ, ppm: 207.0; 175.6; 172.3; 163.1; 159.8; 158.5; 157.7; 155.2; 153.7; 153.1; 143.4; 131.4; 131.0; 129.0; 125.2; 121.6; 116.9; 114.4; 113.9; 110.8; 109.9; 77.4; 74.6; 57.4; 55.3; 49.2; 34.7. Found, *m*/*z*: 520.1316 $[M+H]^+$. $C_{27}H_{23}ClFN_4O_4$. Calculated, *m*/*z*: 520.1314.

Molecular docking studies of the synthesized dispiroindolinones 4a–m were performed using the ICM-Pro software (official website: www.molsoft.com) and crystallographic data for proteins that were available in the PDB (official website: www.rcsb.org). For *in silico* modeling, we used crystallographic data obtained for p53–MDM2 in complex with nutlin-3a (4HG7) and (2'*S*,3*R*,4'*S*,5'*R*)-*N*-(2-aminoethyl)-6-chloro-4'-(3-chloro-2-fluorophenyl)-2'-(2,2-dimethylpropyl)-2-oxo-1,2-dihydrospiro[indole-3,3'-pyrrolidine]-5'-carboxamide (PDB code: 4JVR). The predicted active conformations of the reference compounds correlated well with the available crystallographic data of nutlin-3a (4HG7) and 4JVR. For each compound, ≥10 different conformations were generated in ICM-Pro. All conformations from the output were within a particular

range around the minimum of the potential energy. For assessment, we used internal "score" functions calculated automatically in ICM-Pro. All scores and conformations that were generated during modeling were thoroughly analyzed. Of these values, the best score for the conformation that is most closely related to the template supramolecular interface have been selected and represented.

Cytotoxicity and p53 transcriptional reporter activation tests of the synthesized dispiroindolinones 4a–m are described in the Supplementary information file.

X-ray study of compound 4l was performed on a STOE diffractometer with Pilatus100K detector and CuKα radiation (λ 1.54186 Å). Crystallographic data were deposited at the Cambridge Crystallographic Data Center (deposit CCDC 1844112).

Supplementary information file containing ^{1}H and ^{13}C NMR spectra of the synthesized compounds, COSY, NOESY, ^{1}H–^{13}C HSQC, ^{1}H–^{13}C HMBC spectra of compound **4d**, description of the synthesis and analytical data of the starting compounds **2d**,**g**,**i–l** and **3f**,**i**,**k**, HRMS data of compounds **4b–d**,**h–l**, X-ray data of compound **4l**, as well as description of the biological tests is available at the journal website at http://link.springer.com/journal/10593.

This study was supported by Russian Science Foundation (grants 19-03-00201, 19-33-90237, and 18-33-01159).

The authors are thankful to Thermo Fisher Scientific Inc., Textronica AG group (Moscow, Russia), and personally to Prof. Alexander Makarov for providing the Orbitrap Elite mass spectrometer for this work. This work in part of NMR and X-ray structural study was supported by the Lomonosov Moscow State University Program of Development.

References

1. Duffy, M. J.; Synnott, N. C.; Crown, J. *Eur. J. Cancer* **2017**, *83*, 258.
2. Wu, X.; Bayle, J. H.; Olson, D.; Levine, A. J. *Genes Dev.* **1993**, *7*, 1126.
3. Vogelstein, B.; Lane, D.; Levine, A. J. *Nature* **2000**, *408*, 307.
4. Hainaut, P.; Hollstein, M. *Adv. Cancer Res*. **1999**, *77*, 81.
5. Khoo, K. H.; Verma, C. S.; Lane, D. P. *Nat. Rev. Drug Discov.* **2014**, *13*, 217.
6. Graves, B.; Thompson, T.; Xia, M.; Janson, C.; Lukacs, C.; Deo, D.; Di Lello, P.; Fry, D.; Garvie, C.; Huang, K.-S.; Gao, L.; Tovar, C.; Lovey, A.; Wanner, J.; Vassilev, L. T. *Proc. Natl. Acad. Sci. U. S. A.* **2012**, *109*, 11788.
7. Vassilev, L. T.; Vu, B. T.; Graves, B.; Carvajal, D.; Podlaski, F.; Filipovic, Z.; Kong, N.; Kammlott, U.; Lukacs, C.; Klein, C.; Fotouhi, N.; Liu, E. A. *Science* **2004**, *303*, 844.
8. Nguyen, D.; Liao, W.; Zeng, S. X.; Lu, H. *Pharmacol. Ther.* **2017**, *178*, 92.
9. Anil, B.; Riedinger, C.; Endicott, J. A.; Noble, M. E. M. *Acta Crystallogr.*, *Sect. D*: *Biol. Crystallogr.* **2013**, *69*, 1358.
10. Wang, S.; Zhao, Y.; Bernard, D.; Aguilar, A.; Kumar, S. *Protein-Protein Interactions*; Springer: Berlin, Heidelberg, 2012, p. 57.
11. Zhao, Y.; Aguilar, A.; Bernard, D.; Wang, S. *J. Med. Chem.* **2015**, *58*, 1038.
12. Zhao, Y.; Yu, S.; Sun, W.; Liu, L.; Lu, J.; McEachern, D.; Shargary, S.; Bernard, D.; Li, X.; Zhao, T.; Zou, P.; Sun, D.; Wang, S. *J. Med. Chem*. **2013**, *56*, 5553.
13. Beloglazkina, A. A.; Skvortsov, D. A.; Tafeenko, V. A.; Majouga, A. G.; Zyk, N. V.; Beloglazkina, E. K. *Russ. Chem. Bull*., *Int. Ed.* **2018**, *67*, 562. [*Izv. Akad. Nauk*, *Ser. Khim.* **2018**, 562.]
14. Ivanenkov, Y. A.; Vasilevski, S. V.; Beloglazkina, E. K.; Kukushkin, M. E.; Machulkin, A. E.; Veselov, M. S.; Chufarova, N. V.; Chernyagina, E. S.; Vanzcool, A. S.; Zyk, N. V.; Skvortsov, D. A.; Khutornenko, A. A.; Rusanov, A. L.; Tonevitsky, A. G.; Dontsova, O. A.; Majouga, A. G. *Bioorg. Med. Chem. Lett*. **2015**, *25*, 404.
15. Beloglazkina, A. A.; Karpov, N. A.; Mefedova, S. R.; Polyakov, V. S.; Skvortsov, D. A.; Kalinina, M. A.; Tafeenko, V. A.; Majouga, A. G.; Zyk, N. V.; Beloglazkina, E. K. *Russ. Chem. Bull*., *Int. Ed.* **2019**, 1006. [*Izv. Akad. Nauk*, *Ser. Khim.* **2019**, 1006.]
16. Zhao, Y.; Liu, L.; Sun, W.; Lu, J.; McEachern, D.; Li, X.; Yu, S.; Bernard, D.; Ochsenbein, P.; Ferey, V.; Carry, J.-C.; Deschamps, J. R.; Sun, D.; Wang, S. *J. Am. Chem. Soc*. **2013**, *135*, 7223.
17. Hill, R. A.; Connolly, J. D. *Nat. Prod. Rep*. **2015**, *32*, 273.
18. Stilz, H. U.; Guba, W.; Jablonka, B.; Just, M.; Klingler, O.; König, W.; Wehner, V.; Zoller, G. *J. Med. Chem*. **2001**, *44*, 1158.
19. Khodair, A. I. *Carbohydr. Res*. **2001**, *331*, 445.
20. Zaytsev, V. P.; Mertsalov, D. F.; Nadirova, M. A.; Dorovatovskii, P. V.; Khrustalev, V. N.; Sorokina, E. A.; Zubkov, F. I.; Varlamov, A. V. *Chem. Heterocycl. Compd.* **2017**, *53*, 1199. [*Khim. Geterotsikl. Soedin.* **2017**, *53*, 1199.]
21. Guzei, I. A.; Gunn, E. M.; Spencer, L. C.; Schomaker, J. M.; Rigoli, J. W. *CrystEngComm* **2011**, *13*, 3444.
22. Majouga, A. G.; Beloglazkina, E. K.; Vatsadze, S. Z.; Frolova, N. A.; Zyk, N. V. *Russ. Chem. Bull*., *Int. Ed.* **2004**, *53*, 2850. [*Izv. Akad. Nauk*, *Ser. Khim.* **2004**, 2734.]
23. He, J.; Ouyang, G.; Yuan, Z.; Tong, R.; Shi, J.; Ouyang, L. *Molecules* **2013**, *18*, 5142.
24. Kumar, R. R.; Perumal, S.; Senthilkumar, P.; Yogeeswari, P.; Sriram, D. *Tetrahedron* **2008**, *64*, 2962.
25. Beloglazkina, E. K.; Vatsadze, S. Z.; Majouga, A. G.; Frolova, N. A.; Romashkina, R. B.; Zyk, N. V.; Moiseeva, A. A.; Butin, K. P. *Russ. Chem. Bull*., *Int. Ed.* **2005**, *54*, 2771. [*Izv. Akad. Nauk*, *Ser. Khim*. **2005**, 2679.]
26. Ferrari, M.; Fornasiero, M. C.; Isetta, A. M. *J. Immunol. Methods* **1990**, *131*, 165.
27. Tang, J.-J.; Li, J.-G.; Qi, W.; Qiu, W.-W.; Li, P.-S.; Li, B.-L.; Song B.-L. *Cell Metab*. **2011**, *13*, 44.
28. Yu, F.; Wang, Q.; Zhang, Z.; Peng, Y.; Qiu, Y.; Shi, Y.; Zheng, Y.; Xiao, S.; Wang, H.; Huang, X.; Zhu, L.; Chen, K.; Zhao, C.; Zhang, C.; Yu, M.; Sun, D.; Zhang, L.; Zhou, D. *J. Med. Chem*. **2013**, *56*, 4300.
29. Król, S. K.; Kiełbus, M.; Rivero-Müller, A.; Stepulak, A. *BioMed Res. Int.* **2015**. http://dx.doi.org/10.1155/2015/584189
30. Kravchenko, J. E.; Ilyinskaya, G. V.; Komarov, P. G.; Agapova, L. S.; Kochetkov, D. V.; Strom, E.; Frolova, E. I.; Kovriga, I.; Gudkov, A. V.; Feinstein, E.; Chumakov, P. M. *Proc. Natl. Acad. Sci. U. S. A.* **2008**, *105*, 6302.
31. Korohoda, M. J. *Pol. J. Chem*. **1980**, *54*, 683.